JOC The Journal of Organic Chemistry

Article

pubs.acs.org/joc

Mechanism of Nickel-Catalyzed Selective C−N Bond Activation in Suzuki-Miyaura Cross-Coupling of Amides: A Theoretical Investigation

Liu (Leo) Liu,[†] Peng Chen,[†] Ying Sun,[†] Yile Wu,[†] Su Chen,[†] Jun Zhu,*[,‡] and Yufen Zhao*[,†]

[†]Department of Chemistry, College of Chemistry and Chemical Engineering, Key Laboratory for Chemical Biology of Fujian Province and [‡]State Key Laboratory of Physical Chemistry of Solid Surfaces and Fujian Provincial Key Laboratory of Theoretical and Computational Chemistry, College of Chemistry and Chemical Engineering, Xiamen University, Xiamen, 361005 Fujian, China

Supporting Information

ABSTRACT: In textbooks, the low reactivity of amides is attributed to the strong resonance stability. However, Garg and co-workers recently reported the Ni-catalyzed activation of robust amide C−N bonds, leading to conversions of amides into esters, ketones, and other amides with high selectivity. Among them, the Ni-catalyzed Suzuki-Miyaura coupling (SMC) of *N*-benzyl-*N*-tert-butoxycarbonyl (*N*-Bn-*N*-Boc) amides with pinacolatoboronate (PhBpin) was performed in the presence of K_3PO_4 and water. Water significantly enhanced the reaction. With the aid of density functional theory (DFT) calculations, the present study explored the mechanism of the aforementioned SMC reaction as well as analyzed the weakening of amide C−N bond by *N*-functionalization. The most favorable pathway includes four basic steps: oxidative addition, protonation, transmetalation, and reductive elimination. Comparing the base- and water-free process, the transmetalation step with the help of K_3PO_4 and water is significantly more facile. Water efficiently protonates the basic N(Boc) (Bn) group to form a neutral HN(Boc) (Bn), which is easily removed. The transmetalation step is the rate-determining step with an energy barrier of 25.6 kcal/mol. Further, a DFT prediction was carried out to investigate the full catalytic cycle of a cyclic (amino) (aryl)carbene in the Ni-catalyzed SMC of amides, which provided clues for further design of catalysts.

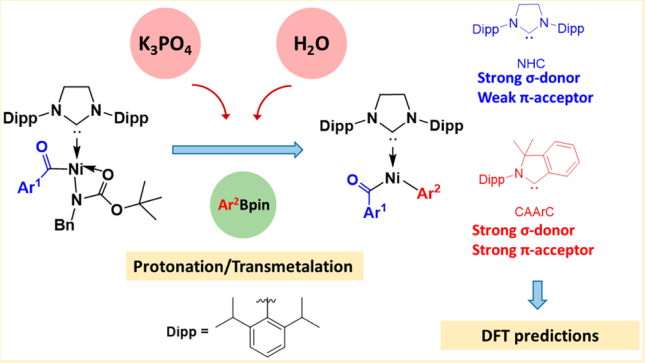

INTRODUCTION

Activation of strong chemical bond is a fascinating topic. The C−N bond is one of the most crucial and ubiquitous chemical bonds, which exists in a number of chemicals ranging from small molecules (e.g., amines and amides) to biomacromolecules (e.g., protein).[1] The amide C−N bond is well-known to be fairly inert under a variety of reaction conditions owing to resonance stabilization,[1a,2] thereby giving rise to the difficulty of modification of amide C−N bond. Enzymes have been found to be capable of breaking amide linkages in nature.[3] However, synthetically, widely used functionalization of amide C−N bonds mainly involved in the transformation of amides to aldehydes[4] or electrophilic intermediates,[5] which could be further modified. These traditional methods usually suffer from relatively strict reaction conditions and low selectivity (e.g., the corresponding alcohols and amines as byproducts).

The direct metal-catalyzed activation of robust amide C−N bonds is a long-standing target for chemists.[6] Gratifyingly, it was achieved by Garg, Houk, and co-workers in 2015. They successfully developed the Ni-catalyzed selective activation and conversion of amides into esters in a one-step process,[7] marking a milestone in direct amide-to-ester transformations. Following this, Garg et al. reported the Ni-catalyzed SMC of amides,[8a] Ni-catalyzed alkylation of amide derivatives[8b] and the Ni-catalyzed two-step conversion of one amide to another.[8c] These important breakthroughs not only offer new synthetic protocols for the conversion of amides to other valuable compounds, but also demonstrate the powerful and fascinating ability of nonprecious transition metals for highly selective cleavage of traditionally "inert" chemical bonds. Independently, the groups of Szostak[9] and Zou[10] showed Pd-catalyzed direct acylative Suzuki couplings of geometrically distorted cyclic imides and arylated mixed imides, respectively. Szostak and co-workers investigated a new generic mode of activation of amide C−N bonds in twisted amides by geometric distortion.[11]

In the Ni-catalyzed SMC of amides,[8a] *N*-Bn-*N*-Boc amide could be efficiently converted into the corresponding ketone in the presence of PhBpin with $Ni(cod)_2$/SIPr as the catalytic system at 50 °C (Figure 1, top). On the basis of the previous reports of Ni-catalyzed cross-coupling reactions,[7,12,13] a possible mechanism has been proposed (Figure 1, bottom), involving three basic steps: oxidative addition, transmetalation, and reductive elimination. The selective C−N bond activation of

Received: August 25, 2016
Published: November 3, 2016

DOI: 10.1021/acs.joc.6b02093
J. Org. Chem. 2016, 81, 11686−11696

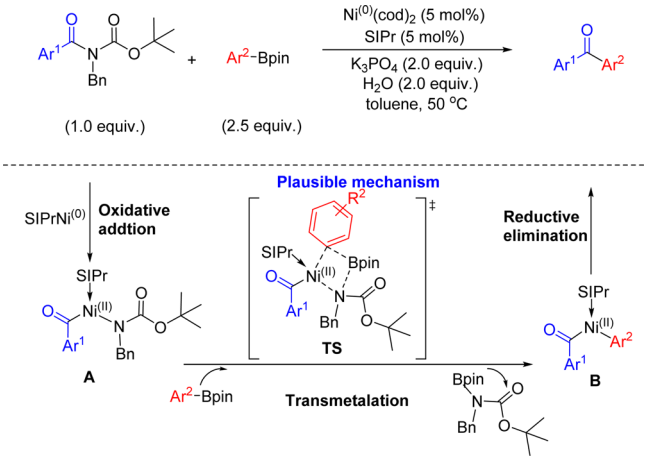

Figure 1. Ni-catalyzed SMC of amides and plausible mechanism.

amides occurs to obtain intermediate **A**. Subsequent transmetalation via a four-membered transition state **TS** gives intermediate **B**, which undergoes the reductive elimination to provide the experimentally observed cross-coupling product. Although the aforementioned mechanisms are plausible, many important details have not been investigated. These include the following: (i) which species is the resting state in the catalytic cycle? (ii) Which step is the rate-determining step? (iii) Why does oxidative addition take place selectively? (iv) What is the crucial role of the base and water? Therefore, we have used DFT calculations to explore the mechanisms in depth. Our results provide hints for further design of transition metal catalysts, which could activate other "inert" chemical bonds.

COMPUTATIONAL METHODS

All the DFT calculations were performed with the Gaussian 09 software package.[14] Optimizations of structures with frequency calculations were carried out with the M06 functional,[15] and a mixed basis set employing D95v(d)[16] for C, H, B, N, and O and LANL2DZ[17] for P, K, and Ni was used. Polarization functions were added for P (ξ_d = 0.387) and Ni (ξ_f = 3.130).[18] Transition states with only one imaginary frequency were examined by vibrational analysis and then submitted to intrinsic reaction coordinate (IRC)[19] calculations to ensure that such structures indeed connected two minima. Energies in solution (toluene) were calculated by means of single-point calculations (IEF-PCM method with the Bondi radii)[20] with the same functional using the SDD[21] pseudopotential for Ni and the extended 6-311++G(2d,p)[22] basis set for the other atoms. The gas-phase geometry was used for all of the solution-phase calculations. A similar treatment was also used in many recent computational studies.[23] The free energy correction from the frequency calculation was added to the single-point energy to obtain the free energy in solution. All of the solution-phase free energies reported herein correspond to the reference state of 1 mol/L, 298 K. The bond dissociation energies (BDEs) were calculated at the M06/6-311++G(2d,p) level of theory in the gas-phase. Natural bond orbital (NBO) calculations were carried out using the NBO 5.9 program[24] at the M06/6-311++G(2d,p)//M06/D95v(d) level of theory. Optimized structures were visualized by the CYLview program[25] or Chemcraft.[26]

RESULTS AND DISCUSSION

Strong Bonds Made Weaker: Weakening of Amide C−N Bond. In the experiments, the *N*-Boc-activated secondary amides were found to be the best reaction partners.[8a] For a better understanding of the preactivation of amide C−N bond, natural bond orbital (NBO) calculations at the M06/6-311++G(2d,p) level of theory were carried out. Figure 2a depicts the resonance structures of amides, showing the resonance stability. The second-order perturbation theory of the NBO method demonstrates a significantly strong π-electron delocalization from the p-type N lone pair to the polar C−O π^* antibond with a donor−acceptor stabilization energy $E^{(2)}$ of 67.0 kcal/mol (Figures 2b and 2d, entry 1). Selected natural localized molecular orbital (NLMO) is shown in Figure 2c, which displays the highly delocalized π bond contributions from the nitrogen atom (84.3% at N, 8.9% at C, and 3.6% at O; $R^1 = R^2 = R^3$ = Me). It is interesting to note that the donor−acceptor stabilization energy $E^{(2)}$ of α-alkyl amide (67.0 kcal/mol; Figure 2d, entry 1) is much higher than that of α-aryl amide (33.7 kcal/mol; Figure 2d, entry 2), indicating α-aryl substituents could weaken the amide C−N bond. Accordingly, the amide bond dissociation energy (BDE) of α-alkyl amide (89.2 kcal/mol) is slightly higher than that of α-aryl amide (86.7 kcal/mol). Furthermore, the substituents at the nitrogen atom of the amide bond are crucial. The π-electron-withdrawing Boc group could efficiently prevent the donation from the N lone pair to the amide polar C−O π^* antibond, leading to a weaker amide C−N bond (Figure 2d, entries 3−4).

In a brief summary, the amide C−N bond of the *N*-Bn-*N*-Boc α-phenyl amide (Figure 2d, entry 4) has been preactivated due to the weakening of n(N)-π^*(C−O) hyperconjugation,

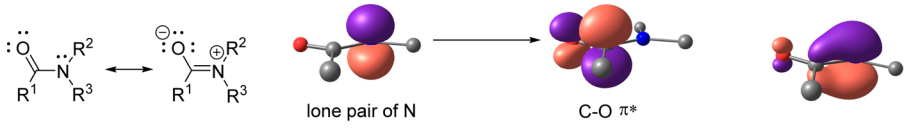

entry	amide	$E^{(2)}$	amide bond energy
1	$R^1 = R^2 = R^3$ = Me	67.0	89.2
2	R^1 = Ph, $R^2 = R^3$ = Me	33.7	86.7
3	R^1 = Me, R^2 = Boc, R^2 = Bn	41.4	86.9
4	R^1 = Ph, R^2 = Boc, R^3 = Bn	24.3	85.7

(d)

Figure 2. (a) The resonance structures of amide. (b) Donor NBO (lone pair of N) and acceptor NBO (C−O π^*) for the second-order perturbation theory analysis. (c) Selected NLMO. (d) Stabilization energy $E^{(2)}$ (kcal/mol) from the second-order perturbation theory analysis. Amide bond energies are given in kcal/mol.

DOI: 10.1021/acs.joc.6b02093
J. Org. Chem. 2016, 81, 11686−11696

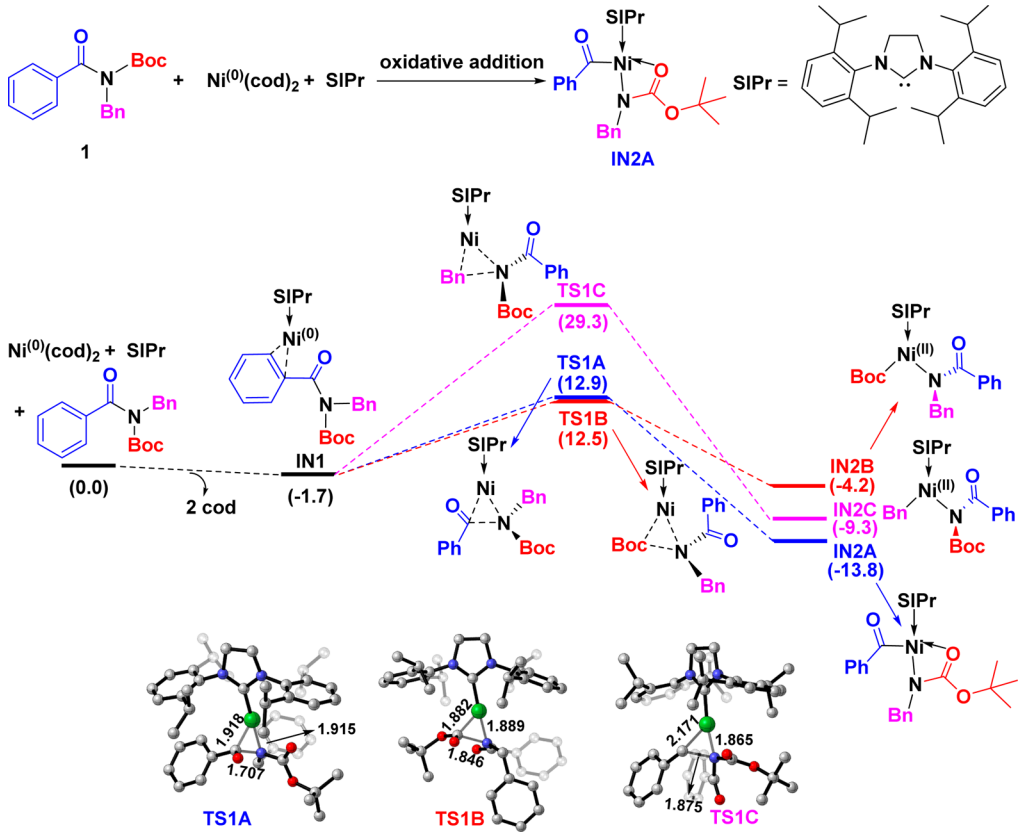

Figure 3. Free energy profile (kcal/mol) for the oxidative addition step of Ni-catalyzed SMC of amides. In the 3D structures, selected bond lengths are given in angstroms.

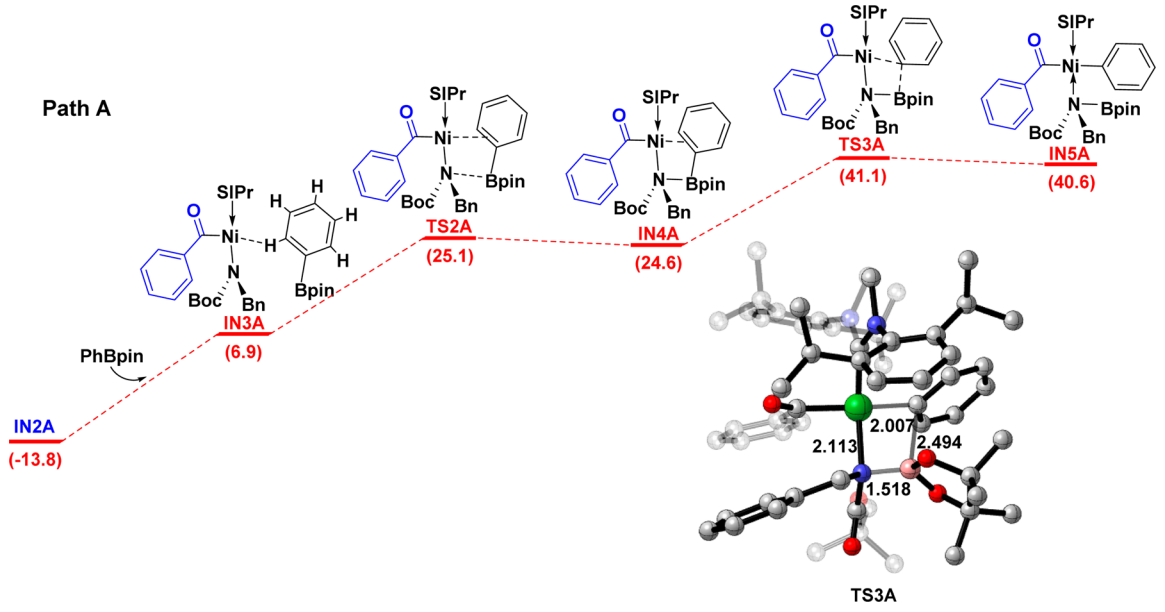

Figure 4. Free energy profile (kcal/mol) for the base- and water-free transmetalation step (Path A) of Ni-catalyzed SMC of amides.

presumably making the next oxidative addition less energy-demanding.

Oxidative Addition: Thermodynamically Favored Chemoselectivity of Amide C–N Activation. In this section, the oxidative addition of $Ni^{(0)}(cod)_2$/SIPr with *N*-Boc-activated secondary amide **1** was investigated (Figure 3). In the experiments, catalytic $Ni(cod)_2$ (5%) and SIPr (5%) were identified in a molar ratio of 1:1. We assume that an η^2 intermediate **IN1** (−1.7 kcal/mol) is formed initially via ligand exchange, where the SIPr ligand and amide **1** coordinate to $Ni^{(0)}$. Note that there are three C–N bonds in **IN1** that can be activated. Thus, we have explored the plausible reaction pathways that involve the activation of C(O)–N, Boc–N, and Bn–N bonds.

Three concerted transition states (Figure 3, bottom) were located involving the cleavage of C(O)–N (**TS1A**), Boc–N

DOI: 10.1021/acs.joc.6b02093
J. Org. Chem. 2016, 81, 11686–11696

(**TS1B**), and Bn−N (**TS1C**) bonds of **IN1**, leading to the formation of **IN2A**, **IN2B**, and **IN2C**, respectively. The free energies of **TS1A** (12.9 kcal/mol) and **TS1B** (12.5 kcal/mol) are much lower than that of **TS1C** (29.3 kcal/mol). Therefore, the activation of the Bn−N bond is kinetically unfavorable to take place.

It is important to understand why no cross-coupling product from the Boc−N activation was observed experimentally, given that the very small energetic difference between **TS1A** and **TS1B**. The IRC calculations reveal that a tetracoordinated intermediate **IN2A** (−13.8 kcal/mol) is formed via **TS1A**, whereas a much less stable tricoordinated **IN2B** (−4.2 kcal/mol) is generated via **TS1B**. As a result, the barrier from **IN2A** to **TS1A** is 26.7 kcal/mol, which is 10.0 kcal/mol higher than that (16.7 kcal/mol) from **IN2B** to **TS1B**. This indicates that oxidative addition of Boc−N to $Ni^{(0)}$ is a readily reversible process, whereas it is an irreversible process for oxidative addition of C(O)−N to $Ni^{(0)}$. Overall, the formation of **IN2A** is thermodynamically and kinetically favored. These results explain why the cross-coupling product from the C(O)−N activation was solely generated.

Transmetalation: Key Role of the Base and Water. We next turned our attention to the transmetalation step. Experimentally, conversion into the desired ketone product was not observed without the presence of K_3PO_4. Moreover, water (2 equiv) could efficiently promote the reaction.[8a] To understand the key role of the base (in this case K_3PO_4) and water, we first investigated the base- and water-free transmetalation (Figure 4, path A). The approach of PhBpin toward **IN2A** generates the complex **IN3A** (6.9 kcal/mol) by the agostic interaction of Ni center and the H atom of phenyl group of PhBpin. Subsequently an intermediate **IN4A** (24.6 kcal/mol) is formed with the lone pair of N and π bond of phenyl group coordinated to B and Ni centers, respectively. Finally, a very late four-membered ring transition state **TS3A** occurs with the cleavage of C−B bond, leading to the formation of a thermodynamically highly unstable species **IN5A** (40.6 kcal/mol), where the phenyl group becomes exclusively bonded to Ni. The energy of **TS3A** (41.1 kcal/mol) is 54.9 kcal/mol higher than that (−13.8 kcal/mol) of **IN2A**. Evidently, these results demonstrate that the transmetalation would not take place in the absence of base and water, in line with the experimental observations.

In Pd- and Ni-catalyzed reactions, many studies have shown that the base played a crucial role in the transmetalation step.[13,27] For example, in the thorough DFT calculations of Ni-catalyzed SMC reactions of aryl esters, Liu et al.[13a] and Houk, Snieckus, Garg et al.[13b] independently reported that the active species in the transmetalation step were borate anions ($ArB(OH)_3^-$) generated in situ from arylboronic acid, water, and K_3PO_4. Shi et al. observed the formation of borate from aryloxylate and boronic acid derivatives.[13c] It is important to note that very recently three pretransmetalation intermediates in the Pd-catalyzed SMC reaction, featuring Pd−O−B linkages, were observed and characterized using low-temperature rapid injection nuclear magnetic resonance spectroscopy by Denmark and Thomas,[28a] which could subsequently transfer their boron-bonded aryl groups to a coordinatively unsaturated Pd center. Additionally, we proposed a new borophosphate species that may participate in the transmetalation step.[13d]

On the basis of the above analysis, the interaction between PhBpin and K_3PO_4 should exist in equilibrium with the corresponding adduct **A1** (Figure 5, top), while in the presence

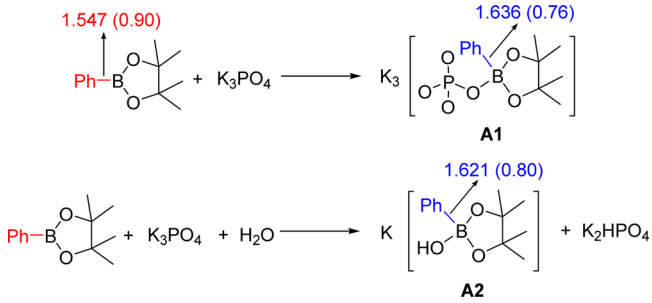

Figure 5. Formation of possible active species **A1** and **A2** that may be involved in the transmetalation step of the Ni-catalyzed SMC of amides. Bond lengths are given in Å. WBIs are given in parentheses.

of water, KPhBpinOH **A2** could be formed coupled with K_2HPO_4 (Figure 5, bottom).[28] The calculations reveal that the C−B bonds in both **A1** (1.636 Å) and **A2** (1.621 Å) have elongated compared with that (1.547 Å) of PhBpin, thus resulting in the weakening of C−B bonds, which is supported by the Wiberg bond indices (WBIs) of C−B bonds (A1:0.76, A2:0.80, PhBpin: 0.90).

Considering that a free charged species hardly exists in less polar organic solvents like toluene, neutral species **A1** and **A2** were selected as the model active species, which would be involved in the catalytic cycle to carry on the transmetalation step. In addition, as we,[13d] Suzuki and Miyaura,[29] Percec,[30] Han,[31] and Fu[32] have proposed that the phosphate anion may coordinate to the metal center in some transition metal catalysis, we proposed six plausible pathways for this process (Figure 6, Paths B−G).

Initially, the dissociation of the carbonyl oxygen of Boc group in **IN2A** occurs to provide a vacant site, simultaneously facilitating **A1** or **A2** coordination. In the paths B and C (Figures 6 and 7), two transition states with the direct C−B bond cleavage/Ni−C bond formation, **TS2B** (23.3 kcal/mol) and **TS2C** (26.8 kcal/mol), are located when **A1** and **A2** approach **IN2A** (−13.8 kcal/mol), respectively. The lengths of C−B bonds in **TS2B** (2.215 Å) and **TS2C** (2.142 Å) are much longer than that (1.547 Å) of PhBpin (Figures 5 and 7). The high overall activation barriers (37.1 and 40.6 kcal/mol, relative to **IN2A**) indicate the difficulty of proceeding for both paths B and C, especially under the experimental conditions (50 °C and 24 h in toluene).[33]

Since the −N(Boc) (Bn) group in **IN2A** could combine with K^+ from **A1** or **A2** followed by removal of a KN(Boc) (Bn) salt, we examined the possibility of paths D and E (Figures 6 and 8), including two basic steps (salt metathesis and C−B bond cleavage). Efforts were made to identify a transition state involving the salt metathesis but all attempts failed. However, the significantly unstable intermediates **IN3D** (23.1 kcal/mol) and **IN3E** (19.4 kcal/mol), containing Ni−O−B linkages, suggest that these steps are thermodynamically unfavorable. Moreover, although the barriers for the subsequent cleavage steps from **IN3D** and **IN3E** are only 13.4 and 12.5 kcal/mol, the overall barriers are 50.3 (**IN2A→TS2D**) and 45.7 kcal/mol (**IN2A→TS2E**), respectively, implying that paths D and E are highly impossible. The high energies of both **TS2D** (36.5 kcal/mol) and **TS2E** (31.9 kcal/mol) might be mainly attributed to the ring strains of the four-membered ring transition states. Note that in path D there are four P-bearing oxygen atoms that can bond to the Ni center. However, in careful searches starting

DOI: 10.1021/acs.joc.6b02093
J. Org. Chem. 2016, 81, 11686−11696

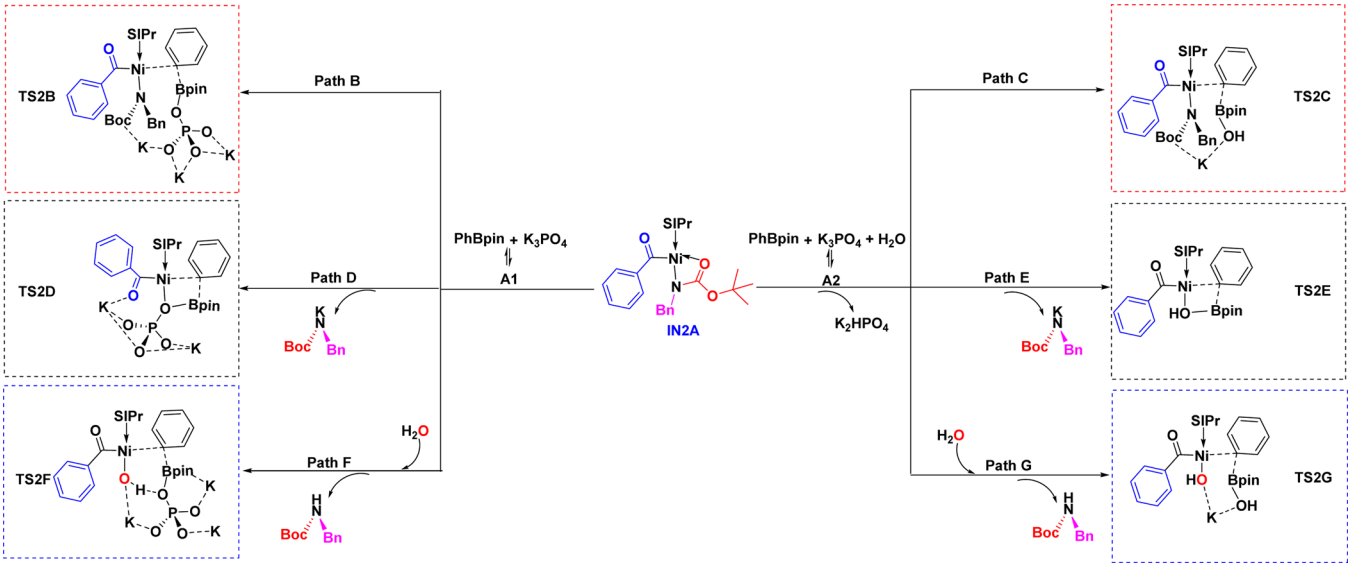

Figure 6. Six plausible pathways for the base- and water-assisted transmetalation step of Ni-catalyzed SMC of amides.

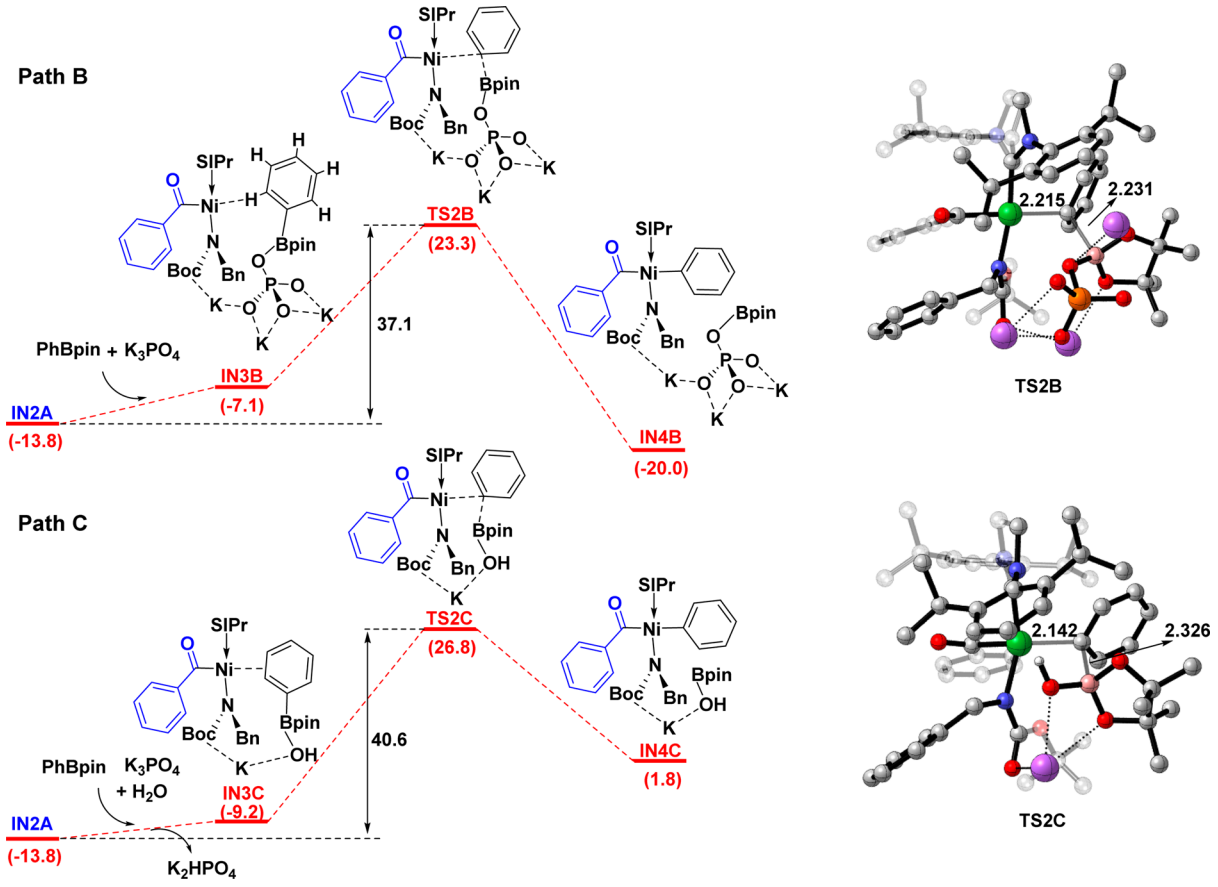

Figure 7. Free energy profile (kcal/mol) for the base- and water-assisted transmetalation steps (Paths B and C) of Ni-catalyzed SMC of amides. Bond lengths are given in Å.

from various isomers, we found that the free energy of **TS2D** is the lowest (See the Supporting Information for details).

Water is known to participate in the cross-coupling catalytic process.[13b,34] Shi and co-workers[34a] reported that the amount of water plays an essential role in promoting the transformation step of Ni-catalyzed C−O activation of phenolic carboxylates. Garg, Snieckus, Houk, and co-workers[13b] showed that water can coordinate to Ni, which thus stabilizes the resting state of Ni-carbamate catalyst. Inspired by the intriguing results, paths F and G were explored (Figures 6, 9, and 10), in which water can coordinate to the Ni center of **IN2A**, followed by protonation of −N(Boc) (Bn). After release of HN(Boc) (Bn), transition states involving C−B bond cleavage/Ni−C bond formation would take place to complete the transmetalation step.

Figure 9 depicts the free energy profile for the water- and K_3PO_4-assisted transmetalation step. First, the approach of a

DOI: 10.1021/acs.joc.6b02093
J. Org. Chem. 2016, 81, 11686−11696

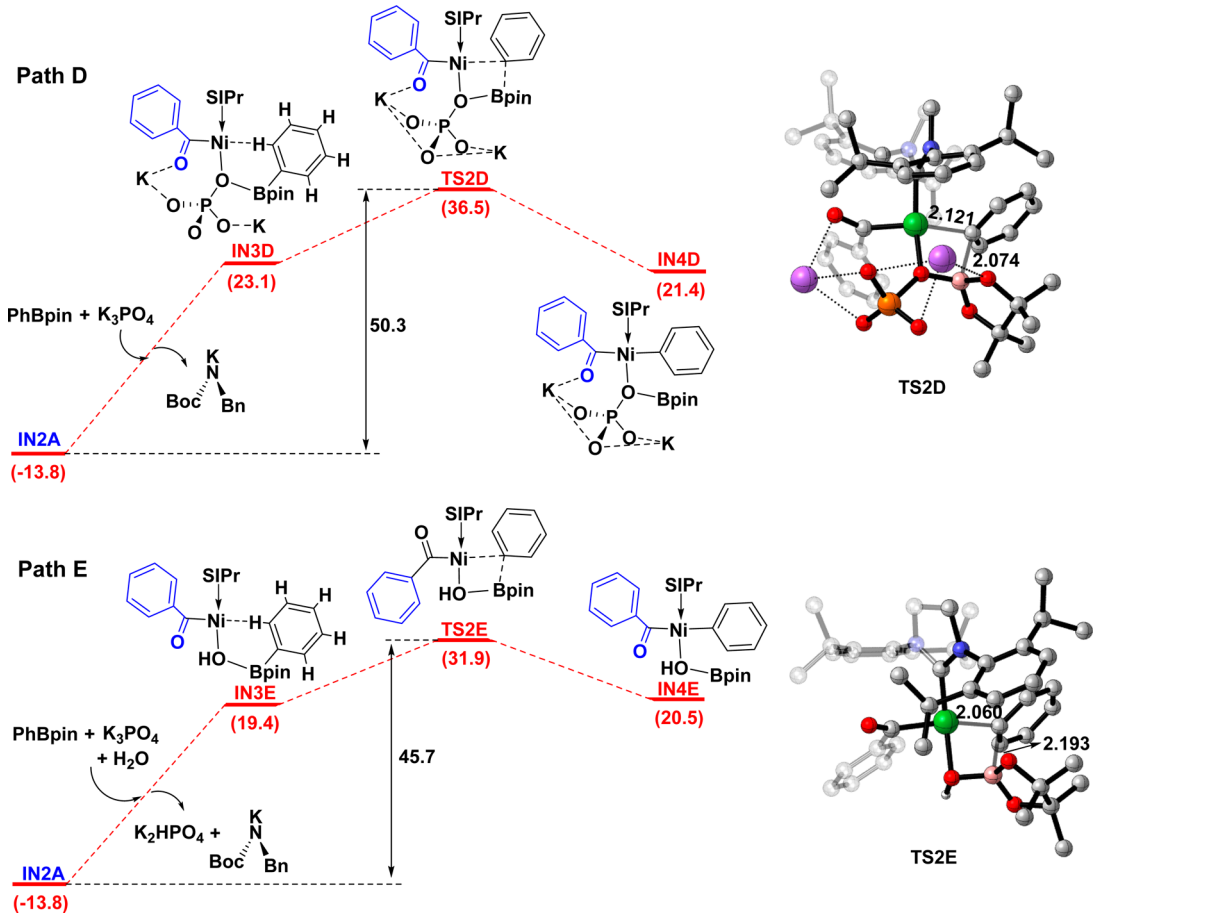

Figure 8. Free energy profile (kcal/mol) for the base- and water-assisted transmetalation steps (Paths D and E) of Ni-catalyzed SMC of amides. Bond lengths are given in Å.

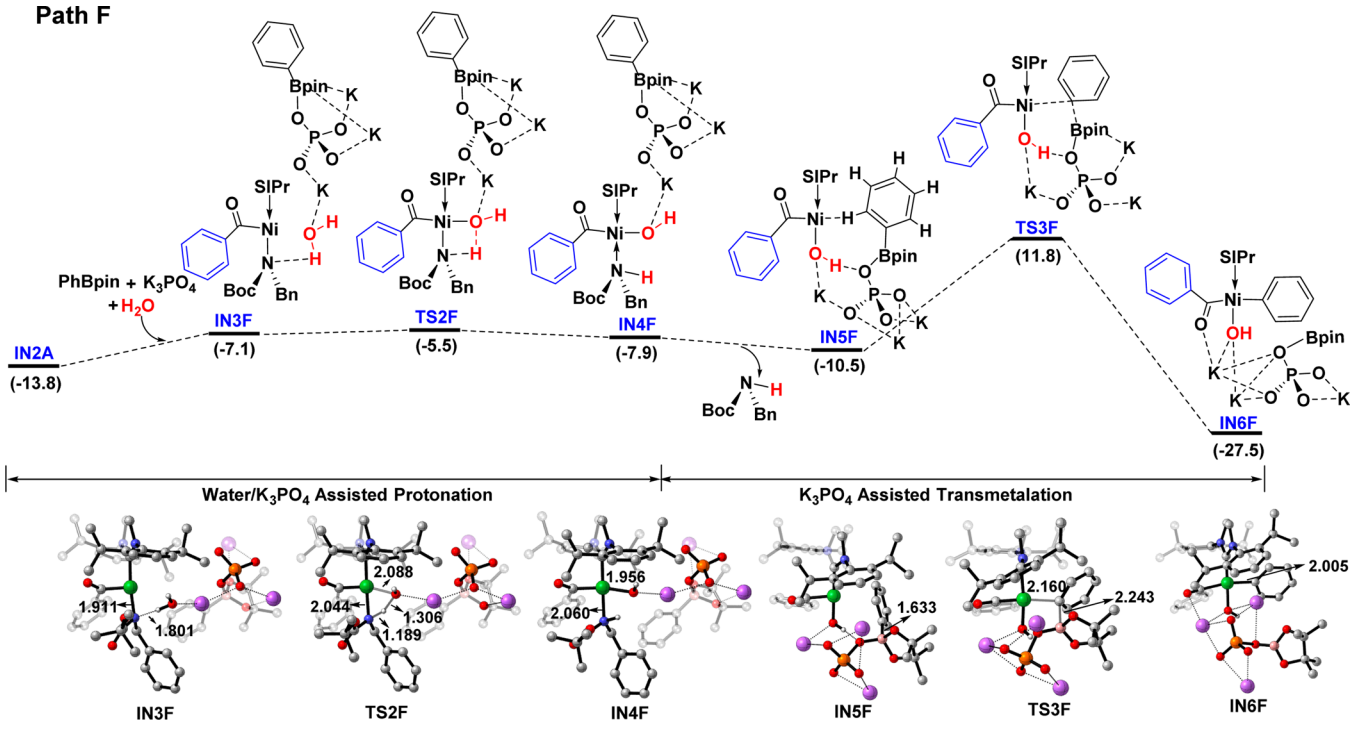

Figure 9. Free energy profile (kcal/mol) for the water- and K_3PO_4-assisted transmetalation step (Path F) of Ni-catalyzed SMC of amides. Bond lengths are given in Å.

DOI: 10.1021/acs.joc.6b02093
J. Org. Chem. 2016, 81, 11686−11696

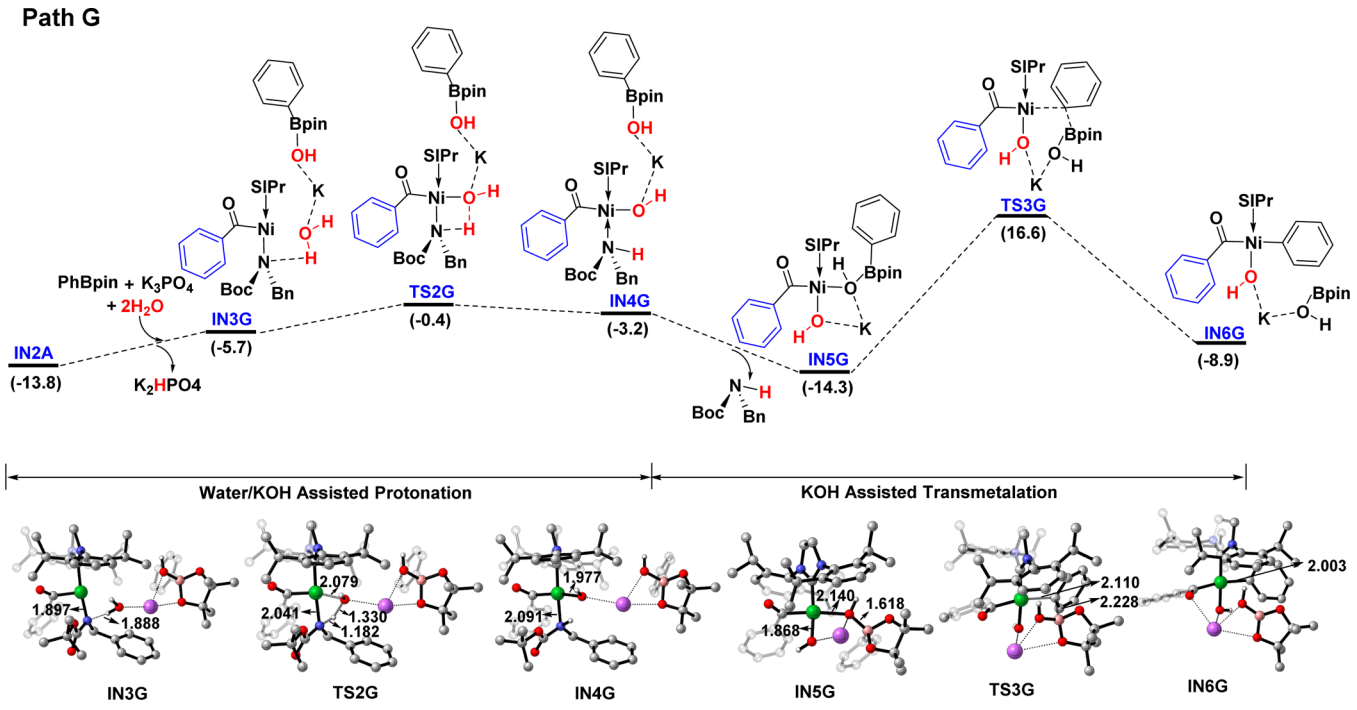

Figure 10. Free energy profile (kcal/mol) for the water- and KOH-assisted transmetalation step (Path G) of Ni-catalyzed SMC of amides. Bond lengths are given in Å.

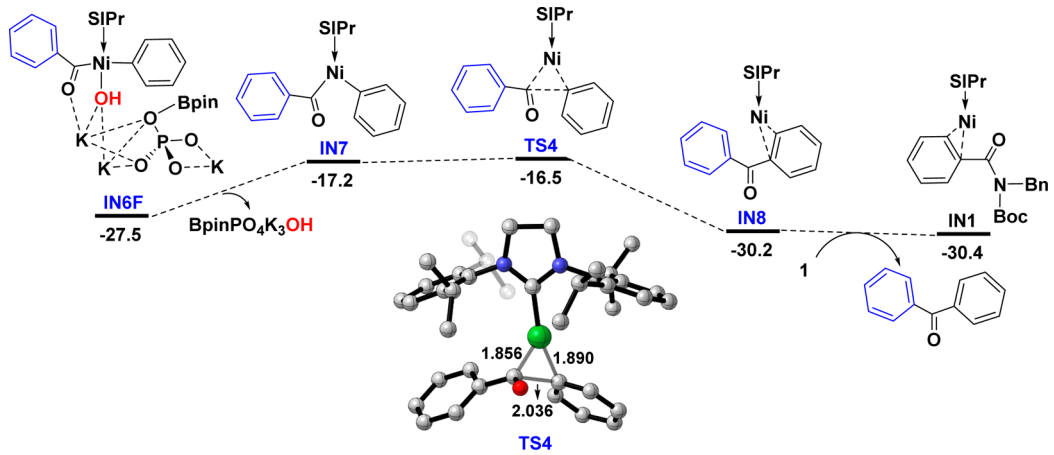

Figure 11. Free energy profile (kcal/mol) for the reductive elimination step of Ni-catalyzed SMC of amides. Bond lengths are given in Å.

water molecule complexed with **A1** toward **IN2A** results in the formation of an intermediate **IN3F** (−7.1 kcal/mol), where one of the O−H bonds of water binds with nitrogen atom of N(Boc) (Bn) via a hydrogen bond (1.801 Å). Next, a very facile protonation step occurs with a four membered ring transition state **TS2F** (−5.5 kcal/mol), involving the cleavage of O−H bond and the formation of both N−H and Ni−O bonds. In the ensuing intermediate **IN4F** (−7.9 kcal/mol), the Ni−N bond (2.060 Å) becomes much longer compared to that (1.911 Å) of **IN3F**, which is an indication of a weakening of the Ni−N bond. Indeed, a more stable intermediate **IN5F** (−10.5 kcal/mol) is formed by the release of a neutral HN(Boc) (Bn) molecule. In **IN5F**, the hydroxyl group is in the trans-position of SIPr ligand. The C−B bond length (1.633 Å) is similar to that (1.636 Å) of **A1** (Figures 5 and 9). Lastly, the K_3PO_4-assisted transmetalation step takes place through a transition state **TS3F** (11.8 kcal/mol) with an overall activation barrier of 25.6 kcal/mol (**IN2A→TS3F**). The final process is highly exergonic, leading to the generation of **IN6F** (−27.5 kcal/mol). Importantly, potassium cations are possibly complexed with the excess water molecules in this transformation. We further modeled the process employing complexation of water and potassium cations (see the Supporting Information for details). However, the results show that the energies in the protonation and transmetalation steps do not differ significantly.

Similarly, the water- and KOH-assisted transmetalation has also been investigated, starting from the removal of a K_2HPO_4 salt (Figures 6 and 10). The activation energies of the protonation and transmetalation are computed to be 13.4 (**IN2A→TS2G**) and 30.9 kcal/mol (**IN5G→TS3G**), respectively. The higher energy [5.3 kcal/mol relative to **TS3F** (11.8 kcal/mol)] of **TS3G** clearly shows that path F is the most favorable process for the transmetalation step of Ni-catalyzed SMC of amides. Additionally, water-assisted transmetalation process with the absence of K_3PO_4 has been investigated,

DOI: 10.1021/acs.joc.6b02093
J. Org. Chem. 2016, 81, 11686−11696

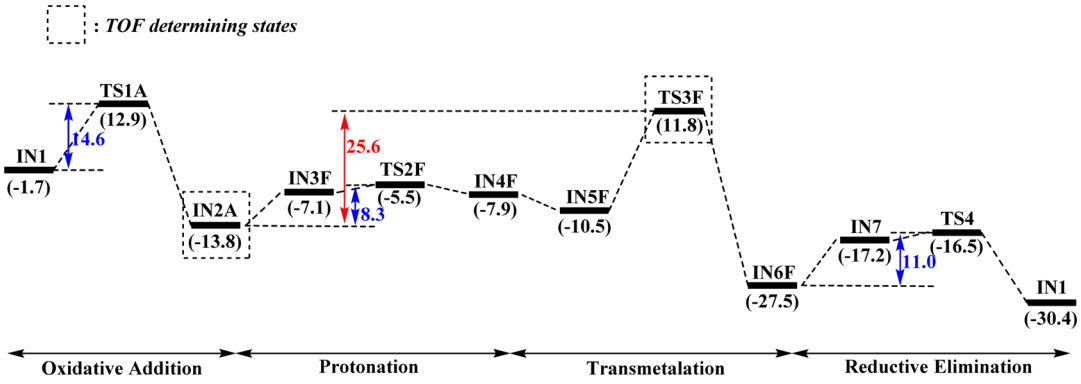

Figure 12. Free energy profile (kcal/mol) for the overall catalytic cycle.

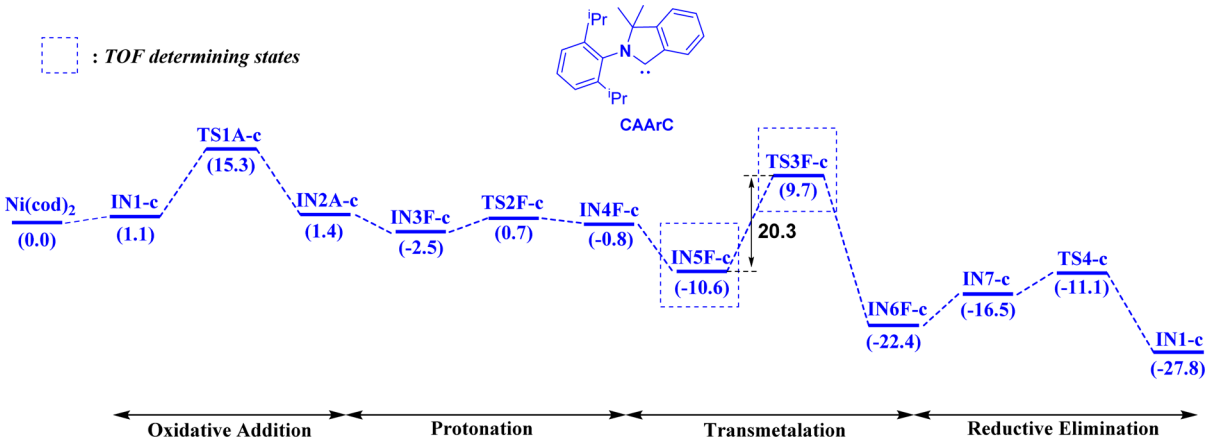

Figure 13. Free energy profile (kcal/mol) using CAArC as the ligand.

showing an activation barrier of 29.9 kcal/mol (see the Supporting Information for details).

According to above analysis, one can realize that the cooperation of water and K_3PO_4 plays a key role in the transmetalation step (Figure 9). Water can efficiently protonate the basic N(Boc) (Bn) group to form a neutral HN(Boc) (Bn) for easy removal. The ensuing hydroxyl together with **A1** can stabilize the intermediate **IN5F** and the transition state **TS3F**, making the transmetalation step easier compared to other pathways (Figures 6−10).

Reductive Elimination: Recycling the Catalytically Active Species IN1. Finally, similar to the reports by Grag and Houk,[7] the reductive elimination step illustrated in Figure 11 is found to be not energy-demanding. After removal of the $BpinPO_4K_3OH$ species, a tricoordinated Ni(II) complex **IN7** (−17.2 kcal/mol) is generated. Subsequently a very early three-membered ring transition state **TS4** with an activation energy of 11.0 kcal/mol (**IN6F** → **TS4**) is identified, which then leads to the formation of a stable Ni(0)-η^2 complex **IN8** (−30.2 kcal/mol). The final product extrusion completes the catalytic cycle to regenerate **IN1**.

Full Catalytic Cycle. As shown in Figure 12, the mechanism of the overall catalytic cycle includes four major steps (oxidative addition, protonation, transmetalation, and reductive elimination). Overall, the rate-determining transition state with the free energy of 11.8 kcal/mol is **TS3F**. The energy barrier of the transmetalation step (rate-determining step) is 25.6 kcal/mol (relative to **IN2A**), which is much higher than those of oxidative addition (14.6 kcal/mol), protonation (8.3 kcal/mol), and reductive elimination (11.0 kcal/mol). Thus, **IN2A** (−13.8 kcal mol^{-1}) is the resting state in the catalytic cycle. The calculation results are in excellent agreement with the experimental observation that the Ni-catalyzed SMC of amides was carried out at 50 °C.[33]

DFT Prediction. *N*-Heterocyclic carbenes (NHCs) and cyclic (alkyl) (amino) carbenes (CAACs) are prominent ligands for transition metals, which has led to a variety of breakthroughs in the field of homogeneous catalysis.[35] For example, the groups of Fürstner,[36] Bertrand,[37] Cazin,[38] and Zeng[37a,39] showed that the π-acceptor properties of carbene ligands influence the outcome of transition-metal-catalyzed reactions. This effect is mainly attributed to the non-negligible π back-donation from the d-electrons of transition metals to the vacant orbital of carbene centers.[40]

Encouraged by recent achievements in theoretical predictions,[41] we evaluated the full catalytic cycle of a cyclic (amino) (aryl)carbene (CAArC)[37a] in Ni-catalyzed SMC of amides computationally. Because the experimentally used SIPr is a strong σ-donor ligand with poor π-accepting ability,[40] a CAArC featuring different property (similar strong σ-donating but enhanced π-accepting ability) was chosen (Figure 13). The energetic span model (ESM) developed by Kozuch and Shaik[42] was employed to analyze full catalytic cycles since the turnover-frequency (TOF) analysis enables the identification of the best catalyst for a given catalytic cycle. Free energies were used to calculate the energy span (δE)[42,43] that serves as the apparent activation energy of catalytic cycle.

According to the ESM, in the case of the SIPr ligand (Figure 12), **TS3F** and **IN2A** are the TOF-determining transition state (TDTS) and TOF-determining intermediate (TDI), respec-

DOI: 10.1021/acs.joc.6b02093
J. Org. Chem. 2016, 81, 11686−11696

tively. The apparent activation energy of the catalytic cycle is 25.6 kcal/mol, which is 5.3 kcal/mol higher than that (20.3 kcal/mol) of the CAArC ligand [Figure 13, **TS3F-c** (TDTS), and **IN5F-c** (TDI)]. This difference corresponds to a relative TOF_{rel}(CAArC/SIPr) of 3.9×10^3, thus suggesting that utilizing the CAArC ligand would result in improved results in the Ni-catalyzed SMC of amides. Note that the relative energy of **IN2A** (−13.8 kcal/mol) is much lower than that (1.4 kcal/mol) of **IN2A-c**, which is the main cause for the difference of the apparent activation energy. Figure 14 depicts the

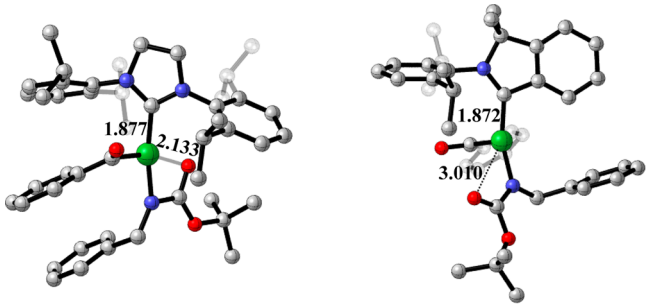

Figure 14. Optimized structures of **IN2A** and **IN2A-c**. Bond lengths are given in Å.

optimized structures of the oxidative addition products **IN2A** and **IN2A-c**, which feature tetracoordinated and tricoordinated Ni(II) centers, respectively. The enhanced π-accepting ability of CAArC superiorly allows to stabilize the low coordinated Ni(II) center of **IN2A-c**,[44] while no stable tricoordinated isomer of **IN2A** could be located using SIPr as the ligand.

CONCLUSION

Ni-catalyzed selective activation of amide C−N bond paves the way for the cross-coupling reactions of amides. Thorough DFT calculations were performed to study the mechanism of the SMC reaction of amides. Not only do the results demonstrate how such interesting reactions proceed, but also provide clues on how to manipulate traditionally inert chemical bonds. First, the NBO analysis suggests that the amide C−N bond of the experimentally used *N*-Bn-*N*-Boc α-phenyl amide has been preactivated due to the weakening of n(N)-π^*(C−O) hyperconjugation.

Second, we show that the overall catalytic cycle of this newly discovered reaction includes four basic steps (oxidative addition, protonation, transmetalation, and reductive elimination). In the oxidative addition step, the Ni-catalyzed selective cleavage of the amide C(O)−N bond is more thermodynamically and kinetically favored, compared with the processes of cleavage of Boc−N and Bn−N bonds. The transmetalation is the rate-determining step with an activation barrier of 25.6 kcal/mol, in which the base K_3PO_4 and water play crucial roles. The basic N(Boc) (Bn) group could be efficiently protonated by water, giving a neutral HN(Boc) (Bn) for easy removal. The ensuing hydroxyl coupled with **A1** enable stabilization of the intermediate **IN5F** and the transition state **TS3F**. The protonation and reductive elimination steps were found to be not energy-demanding.

Lastly, a DFT prediction was carried out to investigate the full catalytic cycle of a CAArC in Ni-catalyzed SMC of amides. On the basis of the ESM, computationally, the CAArC performs better in the Ni-catalyzed SMC of amides. Our results provide hints for further design and development of efficient catalysts, which may have a positive impact on sustainable chemistry.[45]

ASSOCIATED CONTENT

Supporting Information

The Supporting Information is available free of charge on the ACS Publications website at DOI: 10.1021/acs.joc.6b02093.

Calculated energies, free energies of isomers of **TS2D**, free energy profile of water-assisted transmetalation with the absence of K_3PO_4, transmetalation steps using different substituents on N atom, comparison of explicit-solvation and polarizable continuum model, and Cartesian coordinates for all the species (PDF)

AUTHOR INFORMATION

Corresponding Authors

*jun.zhu@xmu.edu.cn

*yfzhao@xmu.edu.cn

ORCID

Liu (Leo) Liu: 0000-0003-4934-0367

Notes

The authors declare no competing financial interest.

ACKNOWLEDGMENTS

We acknowledge financial support from the Chinese National Natural Science Foundation (Grants 21375113, 21232005, 21103142, 21573179, and 21133007), the National Basic Research Program of China (Grants 2012CB821600, 2013CB910700, and 2011CB808504), the Program for New Century Excellent Talents in University (NCET-13-0511), the Fundamental Research Funds for the Central Universities (Grant 2012121021), and the Program for Changjiang Scholars and Innovative Research Team in University (Grant IRT1263). Thanks are also given to Dr. D.A. Ruiz for English improvement.

REFERENCES

(1) (a) *The Amide Linkage: Structural Significance in Chemistry, Biochemistry, and Materials Science*; Greenberg, A., Breneman, C. M., Liebman, J. F., Eds.; Wiley, 2003. (b) Ni, F.; Fu, C.; Gao, X.; Liu, Y.; Xu, P.; Liu, L.; Lv, Y.; Fu, S.; Sun, Y.; Han, D.; Li, Y.; Zhao, Y. *Sci. China: Chem.* **2015**, *58*, 374−382.

(2) Kemnitz, C. R.; Loewen, M. J. *J. Am. Chem. Soc.* **2007**, *129*, 2521−2528.

(3) (a) *Proteases: Structure and Function*; Brix, K., Stöcker, W., Eds.; Springer, 2013. (b) Van Vranken, D. L.; Weiss, G. A. *Introduction to Bioorganic Chemistry and Chemical Biology*; Garland Science, 2013.

(4) (a) Spletstoser, J. T.; White, J. M.; Tunoori, A. R.; Georg, G. I. *J. Am. Chem. Soc.* **2007**, *129*, 3408−3419. (b) Nahm, S.; Weinreb, S. M. *Tetrahedron Lett.* **1981**, *22*, 3815−3818. (c) Bower, S.; Kreutzer, K. A.; Buchwald, S. L. *Angew. Chem., Int. Ed. Engl.* **1996**, *35*, 1515−1516.

(5) (a) Dineen, T. A.; Zajac, M. A.; Myers, A. G. *J. Am. Chem. Soc.* **2006**, *128*, 16406−16409. (b) Evans, D. A.; Carter, P. H.; Dinsmore, C. J.; Barrow, J. C.; Katz, J. L.; Kung, D. W. *Tetrahedron Lett.* **1997**, *38*, 4535−4538. (c) Paik, S.; White, E. H. *Tetrahedron Lett.* **1994**, *35*, 7731−7734. (d) Kaiser, D.; Maulide, N. *J. Org. Chem.* **2016**, *81*, 4421−4428. and references cited therein. (e) Ruider, S. A.; Maulide, N. *Angew. Chem., Int. Ed.* **2015**, *54*, 13856−13858. and references cited therein. (f) Huang, P.-Q.; Huang, Y.-H.; Geng, H.; Ye, J.-L. *Sci. Rep.* **2016**, *6*, 28801.

(6) For reviews of C−N bond activations, see: (a) Wang, Q.; Su, Y.; Li, L.; Huang, H. *Chem. Soc. Rev.* **2016**, *45*, 1257−1272. (b) Ouyang,

K.; Hao, W.; Zhang, W.-X.; Xi, Z. *Chem. Rev.* **2015**, *115*, 12045−12090.
(7) Hie, L.; Fine Nathel, N. F.; Shah, T. K.; Baker, E. L.; Hong, X.; Yang, Y.-F.; Liu, P.; Houk, K. N.; Garg, N. K. *Nature* **2015**, *524*, 79−83.
(8) (a) Weires, N. A.; Baker, E. L.; Garg, N. K. *Nat. Chem.* **2015**, *8*, 75−79. (b) Simmons, B. J.; Weires, N. A.; Dander, J. E.; Garg, N. K. *ACS Catal.* **2016**, *6*, 3176−3179. (c) Baker, E. L.; Yamano, M. M.; Zhou, Y.; Anthony, S. M.; Garg, N. K. *Nat. Commun.* **2016**, *7*, 11554.
(9) Meng, G.; Szostak, M. *Org. Lett.* **2015**, *17*, 4364−4367.
(10) Li, X.; Zou, G. *Chem. Commun.* **2015**, *51*, 5089−5092.
(11) (a) Szostak, R.; Aube, J.; Szostak, M. *Chem. Commun.* **2015**, *51*, 6395−6398. (b) Szostak, R.; Aubé, J.; Szostak, M. *J. Org. Chem.* **2015**, *80*, 7905−7927. (c) Liu, C.; Achtenhagen, M.; Szostak, M. *Org. Lett.* **2016**, *18*, 2375−2378. (d) Meng, G.; Szostak, M. *Org. Lett.* **2016**, *18*, 796−799. (e) Meng, G.; Szostak, M. *Org. Biomol. Chem.* **2016**, *14*, 5690−5707. (f) Shi, S.; Meng, G.; Szostak, M. *Angew. Chem., Int. Ed.* **2016**, *55*, 6959−6963. (g) Hu, F.; Lalancette, R.; Szostak, M. *Angew. Chem., Int. Ed.* **2016**, *55*, 5062−5066. (h) Meng, G.; Szostak, M. *Angew. Chem., Int. Ed.* **2015**, *54*, 14518−14522. (i) Meng, G.; Shi, S.; Szostak, M. *ACS Catal.* **2016**, *6*, 7335−7339. (j) Szostak, R.; Shi, S.; Meng, G.; Lalancette, R.; Szostak, M. *J. Org. Chem.* **2016**, *81*, 8091−8094. For a recent review, see: (k) Liu, C.; Szostak, M. *Chem. - Eur. J.* **2016**, DOI: 10.1002/chem.201605012.
(12) For reviews, see: (a) Han, F.-S. *Chem. Soc. Rev.* **2013**, *42*, 5270−5298. (b) Tollefson, E. J.; Hanna, L. E.; Jarvo, E. R. *Acc. Chem. Res.* **2015**, *48*, 2344−2353. (c) Tobisu, M.; Chatani, N. *Top. Curr. Chem.* **2016**, *374*, 1−28.
(13) (a) Li, Z.; Zhang, S.-L.; Fu, Y.; Guo, Q.-X.; Liu, L. *J. Am. Chem. Soc.* **2009**, *131*, 8815−8823. (b) Quasdorf, K. W.; Antoft-Finch, A.; Liu, P.; Silberstein, A. L.; Komaromi, A.; Blackburn, T.; Ramgren, S. D.; Houk, K. N.; Snieckus, V.; Garg, N. K. *J. Am. Chem. Soc.* **2011**, *133*, 6352−6363. (c) Yu, D.-G.; Shi, Z.-J. *Angew. Chem., Int. Ed.* **2011**, *50*, 7097−7100. (d) Liu, L.; Zhang, S.; Chen, H.; Lv, Y.; Zhu, J.; Zhao, Y. *Chem. - Asian J.* **2013**, *8*, 2592−2595. (e) Hong, X.; Liang, Y.; Houk, K. N. *J. Am. Chem. Soc.* **2014**, *136*, 2017−2025. (f) Hie, L.; Fine Nathel, N. F.; Hong, X.; Yang, Y.-F.; Houk, K. N.; Garg, N. K. *Angew. Chem., Int. Ed.* **2016**, *55*, 2810−2814.
(14) Frisch, M. J.; Trucks, G. W.; Schlegel, H. B.; Scuseria, G. E.; Robb, M. A.; Cheeseman, J. R.; Scalmani, G.; Barone, V.; Mennucci, B.; Petersson, G. A.; Nakatsuji, H.; Caricato, M.; Li, X.; Hratchian, H. P.; Izmaylov, A. F.; Bloino, J.; Zheng, G.; Sonnenberg, J. L.; Hada, M.; Ehara, M.; Toyota, K.; Fukuda, R.; Hasegawa, J.; Ishida, M.; Nakajima, T.; Honda, Y.; Kitao, O.; Nakai, H.; Vreven, T.; Montgomery, J. A.; Peralta, Jr., J. E.; Ogliaro, F.; Bearpark, M.; Heyd, J. J.; Brothers, E.; Kudin, K. N.; Staroverov, V. N.; Keith, T.; Kobayashi, R.; Normand, J.; Raghavachari, K.; Rendell, A.; Burant, J. C.; Iyengar, S. S.; Tomasi, J.; Cossi, M.; Rega, N.; Millam, J. M.; Klene, M.; Knox, J. E.; Cross, J. B.; Bakken, V.; Adamo, C.; Jaramillo, J.; Gomperts, R.; Stratmann, R. E.; Yazyev, O.; Austin, A. J.; Cammi, R.; Pomelli, C.; Ochterski, J. W.; Martin, R. L.; Morokuma, K.; Zakrzewski, V. G.; Voth, G. A.; Salvador, P.; Dannenberg, J. J.; Dapprich, S.; Daniels, A. D.; Farkas, O.; Foresman, J. B.; Ortiz, J. V.; Cioslowski, J.; Fox, D. J. *Gaussian 09*, revision B.01; Gaussian, Inc.: Wallingford CT, 2010.
(15) Zhao, Y.; Truhlar, D. G. *Theor. Chem. Acc.* **2008**, *120*, 215−241.
(16) Dunning, T. H., Jr.; Hay, P. J. In *Modern Theoretical Chemistry*; Schaefer, H. F., III, Ed.; Plenum Press: New York, 1976; Vol. 3, pp 1−28.
(17) Wadt, W. R.; Hay, P. J. *J. Chem. Phys.* **1985**, *82*, 284−298.
(18) (a) Hollwarth, A.; Bohme, M.; Dapprich, S.; Ehlers, A. W.; Gobbi, A.; Jonas, V.; Kohler, K. F.; Stegmann, R.; Veldkamp, A.; Frenking, G. *Chem. Phys. Lett.* **1993**, *208*, 237−240. (b) Ehlers, A.; Böhme, M.; Dapprich, S.; Gobbi, A.; Höllwarth, A.; Jonas, V.; Köhler, K.; Stegmann, R.; Veldkamp, A.; Frenking, G. *Chem. Phys. Lett.* **1993**, *208*, 111−114.
(19) (a) Fukui, K. *J. Phys. Chem.* **1970**, *74*, 4161−4163. (b) Fukui, K. *Acc. Chem. Res.* **1981**, *14*, 363−368.
(20) Bondi, A. *J. Phys. Chem.* **1964**, *68*, 441−451.
(21) Andrae, D.; Haeussermann, U.; Dolg, M.; Stoll, H.; Preuss, H. *Theor. Chim. Acta* **1990**, *77*, 123−141.
(22) (a) Krishnan, R.; Binkley, J. S.; Seeger, R.; Pople, J. A. *J. Chem. Phys.* **1980**, *72*, 650−654. (b) McLean, A. D.; Chandler, G. S. *J. Chem. Phys.* **1980**, *72*, 5639−5648. (c) Clark, T.; Chandrasekhar, J.; Spitznagel, G. W.; Schleyer, P. v. R. *J. Comput. Chem.* **1983**, *4*, 294−301.
(23) (a) Yang, Y.-F.; Houk, K. N.; Wu, Y.-D. *J. Am. Chem. Soc.* **2016**, *138*, 6861−6868. (b) Qi, X.; Zhang, H.; Shao, A.; Zhu, L.; Xu, T.; Gao, M.; Liu, C.; Lan, Y. *ACS Catal.* **2015**, *5*, 6640−6647. (c) Jiang, Y.-Y.; Yan, L.; Yu, H.-Z.; Zhang, Q.; Fu, Y. *ACS Catal.* **2016**, *6*, 4399−4410. (d) Liu, L.; Wu, Y.; Chen, P.; Chan, C.; Xu, J.; Zhu, J.; Zhao, Y. *Org. Chem. Front.* **2016**, *3*, 423−433.
(24) Glendening, E. D.; Badenhoop, J. K.; Reed, A. E.; Carpenter, J. E.; Bohmann, J. A.; Morales, C. M.; Weinhold, F. *Theoretical Chemistry Institute*; University of Wisconsin: Madison, WI, 2009.
(25) Legault, C. Y. *CYLview*, 1.0b; Université de Sherbrooke: Sherbrooke, Quebec, Canada, 2009; www.cylview.org.
(26) Andrienko, G. A.*ChemCraft*, http://www.chemcraftprog.com.
(27) (a) Xue, L.; Lin, Z. *Chem. Soc. Rev.* **2010**, *39*, 1692−1705. (b) Bonney, K. J.; Schoenebeck, F. *Chem. Soc. Rev.* **2014**, *43*, 6609−6638. (c) Carrow, B. P.; Hartwig, J. F. *J. Am. Chem. Soc.* **2011**, *133*, 2116−2119. (d) Li, Z.; Jiang, Y.-Y.; Fu, Y. *Chem. - Eur. J.* **2012**, *18*, 4345−4357. (e) Xu, L.; Chung, L. W.; Wu, Y.-D. *ACS Catal.* **2016**, *6*, 483−493.
(28) (a) Thomas, A. A.; Denmark, S. E. *Science* **2016**, *352*, 329−332. For a review of anion receptor chemistry, see: (b) Gale, P. A.; Howe, E. N. W.; Wu, X. *Chem* **2016**, *1*, 351−422.
(29) (a) Miyaura, N.; Yamada, K.; Suginome, H.; Suzuki, A. *J. Am. Chem. Soc.* **1985**, *107*, 972−980. (b) Miyaura, N.; Suzuki, A. *Chem. Rev.* **1995**, *95*, 2457−2483. (c) Ishiyama, T.; Murata, M.; Miyaura, N. *J. Org. Chem.* **1995**, *60*, 7508−7510.
(30) (a) Percec, V.; Bae, J.-Y.; Hill, D. H. *J. Org. Chem.* **1995**, *60*, 1060−1065. (b) Rosen, B. M.; Quasdorf, K. W.; Wilson, D. A.; Zhang, N.; Resmerita, A.-M.; Garg, N. K.; Percec, V. *Chem. Rev.* **2011**, *111*, 1346−1416.
(31) Chen, G.-J.; Huang, J.; Gao, L.-X.; Han, F.-S. *Chem. - Eur. J.* **2011**, *17*, 4038−4042.
(32) Lu, Q.; Yu, H.; Fu, Y. *J. Am. Chem. Soc.* **2014**, *136*, 8252−8260.
(33) We estimate the barrier value from the Eyring equation, i.e., $k = (k_B T/h)\exp(-\Delta G^{\ddagger}/RT)$, where k is rate constant, k_B is Boltzmann's constant, h is Planck's constant, $\Delta G^{\ddagger}$ is the activation free energy, R is the gas constant, and T is the temperature. Assuming the concentration of each reactant is 1 mol/L and the second-order rate constant k of a reaction whose half-life is 24 h is 1.2×10^{-5} L/mol·s, we obtain $\Delta G^{\ddagger}$ is 26.3 kcal/mol at 50 °C.
(34) For Ni-catalyzed cross-couplings, see: (a) Guan, B.-T.; Wang, Y.; Li, B.-J.; Yu, D.-G.; Shi, Z.-J. *J. Am. Chem. Soc.* **2008**, *130*, 14468−14470. (b) Antoft-Finch, A.; Blackburn, T.; Snieckus, V. *J. Am. Chem. Soc.* **2009**, *131*, 17750−17752. (c) Xing, C.-H.; Lee, J.-R.; Tang, Z.-Y.; Zheng, J. R.; Hu, Q.-S. *Adv. Synth. Catal.* **2011**, *353*, 2051−2059. (d) Jezorek, R. L.; Zhang, N.; Leowanawat, P.; Bunner, M. H.; Gutsche, N.; Pesti, A. K. R.; Olsen, J. T.; Percec, V. *Org. Lett.* **2014**, *16*, 6326−6329. For Pd-catalyzed cross-couplings, see: (e) Lou, S.; Fu, G. C. *Adv. Synth. Catal.* **2010**, *352*, 2081−2084. (f) Dallas, A. S.; Gothelf, K. V. *J. Org. Chem.* **2005**, *70*, 3321−3323. For others, see: (g) Liang, Y.; Zhou, H.; Yu, Z.-X. *J. Am. Chem. Soc.* **2009**, *131*, 17783−17785. (h) Shi, F.-Q.; Li, X.; Xia, Y.; Zhang, L.; Yu, Z.-X. *J. Am. Chem. Soc.* **2007**, *129*, 15503−15512.
(35) (a) Zhukhovitskiy, A. V.; MacLeod, M. J.; Johnson, J. A. *Chem. Rev.* **2015**, *115*, 11503−11532. (b) Soleilhavoup, M.; Bertrand, G. *Acc. Chem. Res.* **2015**, *48*, 256−266. (c) Nelson, D. J.; Nolan, S. P. *Chem. Soc. Rev.* **2013**, *42*, 6723−6753. (d) Hopkinson, M. N.; Richter, C.; Schedler, M.; Glorius, F. *Nature* **2014**, *510*, 485−496. (e) Melaimi, M.; Soleilhavoup, M.; Bertrand, G. *Angew. Chem., Int. Ed.* **2010**, *49*, 8810−8849.
(36) Alcarazo, M.; Stork, T.; Anoop, A.; Thiel, W.; Fürstner, A. *Angew. Chem., Int. Ed.* **2010**, *49*, 2542−2546.

DOI: 10.1021/acs.joc.6b02093
J. Org. Chem. 2016, 81, 11686−11696

(37) (a) Rao, B.; Tang, H.; Zeng, X.; Liu, L.; Melaimi, M.; Bertrand, G. *Angew. Chem., Int. Ed.* **2015**, *54*, 14915−14919. (b) Tolentino, D. R.; Jin, L.; Melaimi, M.; Bertrand, G. *Chem. - Asian J.* **2015**, *10*, 2139−2142. (c) Hu, X.; Martin, D.; Melaimi, M.; Bertrand, G. *J. Am. Chem. Soc.* **2014**, *136*, 13594−13597. (d) Hu, X.; Martin, D.; Bertrand, G. *New J. Chem.* **2016**, *40*, 5993−5996. (e) Romero, E. A.; Jazzar, R.; Bertrand, G. *Chem. Sci.* **2016**, DOI: 10.1039/C6SC02668K.
(38) Bidal, Y. D.; Lesieur, M.; Melaimi, M.; Nahra, F.; Cordes, D. B.; Athukorala Arachchige, K. S.; Slawin, A. M. Z.; Bertrand, G.; Cazin, C. S. J. *Adv. Synth. Catal.* **2015**, *357*, 3155−3161.
(39) Wei, Y.; Rao, B.; Cong, X.; Zeng, X. *J. Am. Chem. Soc.* **2015**, *137*, 9250−9253.
(40) For experimental determination of π-accepting ability of stable carbene ligands, see: (a) Back, O.; Henry-Ellinger, M.; Martin, C. D.; Martin, D.; Bertrand, G. *Angew. Chem., Int. Ed.* **2013**, *52*, 2939−2943. (b) Hansmann, M. M.; Jazzar, R.; Bertrand, G. *J. Am. Chem. Soc.* **2016**, *138*, 8356−8359. (c) Rodrigues, R. R.; Dorsey, C. L.; Arceneaux, C. A.; Hudnall, T. W. *Chem. Commun.* **2014**, *50*, 162−164. (d) Verlinden, K.; Buhl, H.; Frank, W.; Ganter, C. *Eur. J. Inorg. Chem.* **2015**, *2015*, 2416−2425. (e) Vummaleti, S. V. C.; Nelson, D. J.; Poater, A.; Gomez-Suarez, A.; Cordes, D. B.; Slawin, A. M. Z.; Nolan, S. P.; Cavallo, L. *Chem. Sci.* **2015**, *6*, 1895−1904.
(41) For our achievements, see: (a) Liu, L.; Yuan, H.; Fu, T.; Wang, T.; Gao, X.; Zeng, Z.; Zhu, J.; Zhao, Y. *J. Org. Chem.* **2014**, *79*, 80−87. (b) Wang, T.; Sang, S.; Liu, L.; Qiao, H.; Gao, Y.; Zhao, Y. *J. Org. Chem.* **2014**, *79*, 608−617. (c) Liu, L.; Wu, Y.; Wang, Z.; Zhu, J.; Zhao, Y. *J. Org. Chem.* **2014**, *79*, 6816−6822. (d) Liu, L.; Chan, C.; Zhu, J.; Cheng, C.-H.; Zhao, Y. *J. Org. Chem.* **2015**, *80*, 8790−8795. For experimental realization of ref 41d, see: (e) Wu, D.; Ganguly, R.; Li, Y.; Hoo, S. N.; Hirao, H.; Kinjo, R. *Chem. Sci.* **2015**, *6*, 7150−7155. For selected other examples, see: (f) Zhang, X.; Chung, L. W.; Wu, Y.-D. *Acc. Chem. Res.* **2016**, *49*, 1302−1310. (g) Peng, Q.; Paton, R. S. *Acc. Chem. Res.* **2016**, *49*, 1042−1051. (h) Liu, L.; Ruiz, D. A.; Munz, D.; Bertrand, G. *Chem* **2016**, *1*, 147−153.
(42) (a) Kozuch, S.; Shaik, S. *Acc. Chem. Res.* **2011**, *44*, 101−110. (b) Kozuch, S.; Shaik, S. *J. Phys. Chem. A* **2008**, *112*, 6032−6041.
(43) For selected examples of the application of the energetic span model, see: (a) Dudnik, A. S.; Weidner, V. L.; Motta, A.; Delferro, M.; Marks, T. J. *Nat. Chem.* **2014**, *6*, 1100−1107. (b) Chauvier, C.; Tlili, A.; Das Neves Gomes, C.; Thuery, P.; Cantat, T. *Chem. Sci.* **2015**, *6*, 2938−2942. (c) Liu, J.-B.; Sheng, X.-H.; Sun, C.-Z.; Huang, F.; Chen, D.-Z. *ACS Catal.* **2016**, *6*, 2452−2461.
(44) Roy, S.; Mondal, K. C.; Roesky, H. W. *Acc. Chem. Res.* **2016**, *49*, 357−369.
(45) For a recent review, see: Li, C.-J. *Chem* **2016**, *1*, 423−437.

DOI: 10.1021/acs.joc.6b02093
J. Org. Chem. 2016, 81, 11686−11696